A tree-ring based reconstruction of early summer precipitation in southwestern Virginia (1750-1981)

Andria Dawson, David Austin, David Walker, and Valerie Trouet

September 17, 2014

Abstract

In a closed-canopy forest, stand dynamics play an important role in shaping the forest, and it has been hypothesized that dense forests are not sufficiently limited by climate to warrant climate reconstruction. We collected *Quercus prinus* tree-ring data from a dense forest in the Appalachians, and after removal of stand dynamics and age trends we find strong correlations between annual tree growth and early summer precipitation. To strengthen the climate signal, we include additional southeastern US *Quercus prinus* chronologies in a nested principal component analysis (PCA). Correlation between the growth proxy and early summer precipitation was increased through PCA, and assessment of reconstruction skill was favorable. Our May-June precipitation reconstruction was modeled using a Bayesian regression model, which allowed uncertainty to be quantified. The reconstruction covered the period 1750-1981, and extended the instrumental record by 150 years. The reconstruction showed key drought years identified by other regional reconstructions, as well as an 11-year periodicity, possibly related to solar variability.

1 Introduction

Global circulation models project an increase in average global surface temperatures of 1.0 - 3.5 ° C by the end of this century due to continued increases in greenhouse-gas emissions [3, 4]. However the influence of increased radiative forcing on precipitation regimes is not well understood, and this is particularly the case for the southeastern United States (US) . The 24 models used to make predictions about climate change in the Intergovernmental Panel on Climate Change Fourth Assessment Report were not in consensus with respect to drought frequency in this region [3, 5]. Uncertainty in climate projections makes it difficult to predict water and power usage. The ability to do so is crucial because the southeastern US has experienced substantial increases in population and energy consumption over the last decade [5, 6]. It is important that the public and

urban and water planners in the Southeast have access to information regarding climate change projections and mitigation. Through the use of tree-ring based climate reconstructions, we can better understand past precipitation regimes at both decadal- and centennial time-scales and improve projections of future precipitation patterns.

In order to reduce uncertainty in climate model projections and to extend meteorological records further back in time, tree-ring data are commonly used as regional proxies, particularly in regions where drought (e.g. the American Southwest, [7]) or summer temperature (e.g. the European Alps, [8]) is the limiting tree growth factor. However, tree-ring data have also successfully been used for climate reconstructions in temperate climate regions characterized by high humidity such as the eastern US [9–11]. Trees growing in these regions are typically less limited by water availability and thus less sensitive to drought variability than trees in semiarid regions [13]. The amount of environmental variability recorded in tree-ring time series from a certain area thus generally depends on the degree to which environmental factors are limiting tree growth in that area (Fritts et al. 1965). Furthermore, it has traditionally understood that trees in a closed-canopy forest are not limited by climate to the same extent as trees growing on the forest border [12]. Within a dense forest, stand dynamics play an important role in shaping the forest structure through their influence on radial tree growth and tree survival. As these interactions between individuals increase in strength, the climatic influence on tree growth becomes less dominant.

Despite these challenges to capturing a strong climate signal in tree-ring time series from southeastern US forests, numerous studies have identified significant climate-growth relationships [14–16] and several tree-ring based precipitation reconstructions have been developed for the southeastern US. The most prominent of these reconstructions is likely a spring rainfall reconstruction for the past 1000 years based on Bald cypress tree-ring chronologies from North Carolina, South Carolina, and Georgia [36]. Bald cypress trees grow in excessively wet swamps, yet tree growth is strongly positively correlated with spring and early summer precipitation. At drier sites in Virginia, Pan et al. [14] demonstrated for four deciduous species that both annual ring-width and basal area increments were positively correlated with precipitation from the prior summer and autumn, and current summer. They also report negative correlations with air temperature of the

current growing season. Speer et al. [15] found similar correlations between precipitation and temperature and annual tree growth for oak chronologies from closed canopy forests in the Southern Appalachian Mountains.

In this study, we determine the presence of a significant relationship between chestnut oak (*Quercus prinus*; QUPR from here on) annual growth series in the southern Appalachian Mountains and early summer precipitation and develop a regional QUPR tree-ring chronology. We then use the QUPR chronology to reconstruct early summer precipitation using Bayesian methods. Finally, we evaluated the reliability of the reconstruction by comparing it to other verified regional climate reconstructions.

2 Materials and Methods

2.1 Tree ring data

The study site is an Upland Oak-Pine forest located on the north facing slope of Brush Mountain in South-West Virginia (37 ° 22.2' N, 80 ° 14.8' W), with a site elevation of 558 m (BM in Figure 1). This region is classified as either humid continental or mountain temperate, and characterized by warm, humid summers and winters that are predominantly cool with intermittent warm spells. The mean annual precipitation (1901-2010) at the nearby Blacksburg weather station is 1073 mm and the mean annual temperature is 10.9 ° *C*.

The study site supports dominant QUPR trees amongst a canopy of many species, including scarlet oak (*Quercus coccinea*), northern red oak (*Quercus rubra*), red maple (*Acer rubrum*), Virginia pine (*Pinus virginiana*), pitch pine (*Pinus pungens*), and eastern white pine (*Pinus strobus*). Site access was adjacent to the Appalachian trail but the site was selected to minimize human interference. The steepness of this slope suggested that climate may be a limiting growth factor, but the closed canopy and stand density suggested that stand dynamics may also play a significant role in shaping the forest structure [12].

We sampled 56 QUPR trees and collected two increment cores per tree. Samples were dried, mounted, and sanded according to standard procedure [17]. Crossdating was performed based on the list method, which makes use of marker years that signify relatively favorable or unfavorable growth years in a stand [18]. All

samples were measured using a LINTAB measurement stage with 0.01mm precision, and visual crossdating was checked using COFECHA software [19]. We used inter-series correlation, a measure of stand-level signal, and mean sensitivity, to select a total of 76 tree-ring series from 53 trees to be used for site chronology development.

Non-climatic age and stand dynamics related trends were removed from the individual tree-ring series using smoothing splines with a 50 % cutoff at 50 years using ARSTAN software [20]. This method allowed us the flexibility to remove the episodic-like interaction effects from the time series, while retaining the high-frequency climatic variability. Note that as with any filtering technique, inevitably some portion of the climatic signal will be lost through the removal of these non-climatic trends [21]. We here assume that the loss of climatic signal was negligible, and comparison of the detrended time series with climatic data ultimately determined if the strength of the remaining signal was sufficient to perform further analyses. The Brush Mountain site chronology was then calculated by averaging the individually detrended series using a biweight robust mean (Cook and Peters 1997), and will hereafter be referred to as BM.

We computed the expressed population signal (EPS) to measure the common variability in our chronology at an annual resolution. EPS depends on both signal coherence and annual sample-depth, and EPS values that fall below a predetermined cutoff (0.85) indicate that the chronology is not dominated by a coherent signal, and is therefore deemed less than ideal for climate reconstruction [24].

2.2 Principal component analysis

Water availability may not be the primary limiting factor to tree growth in southeastern US sites, but a large sample size may compensate and help to identify the common climate signals despite site and individual variability. In regions that are subject to site heterogeneity, where significant climatic variance cannot be identified for a standard sample size, principal component analysis (PCA) can be an effective means to extract the common signal in multiple sites and thus overcome the lack of strength of climate signal in individual sites [25–27]. Through the application of PCA,, tree-ring data collected from a network of regional sites can be combined to reduce site level noise through the identification of a common climate signal across

sites.

To increase the strength of the precipitation signal in our chronology, we combined the BM chronology with four eastern US *Quercus* chronologies (3 QUPR and 1 *Quercus alba*) in a in a nested singular value decomposition PCA [28, 29] (Table 1, Figs. 1 and 2). These four chronologies extended back to at least 1845 (the length of the BM chronology) and were significantly correlated with regional precipitation anomalies (see below). Tree-ring data for the four *Quercus* sites were downloaded from the International Tree-Ring Database (ITRDB; http://www.ncdc.noaa.gov/paleo/treering.html) and individual ring-width time series were detrended using a smoothing spline with 50% cutoff at 50 years [21], and subsequently used to develop site chronologies. Chronology reliability for each of the four chronologies was assessed based on the mean sensitivity, inter-series correlation, EPS, and the first-order autocorrelation.

We applied a nested PCA approach to make use of the chronologies that extended prior to 1845: we combined the BM chronology with all four *Quercus* chronologies in a first PCA run (PCA_{1845}) and then added a second PCA run (PCA_{1750}) that included only the 3 chronologies that extended back to 1750 (LH, WD, and OC).. For each PCA run, the PCA1 axes explaining the largest amount of common variance were retained for further analysis and were included in a climate correlation analysis. PCA_{1845} and PCA_{1750} resulted in two potential reconstructions with each its own set of skill and accuracy statistics, as described in section 2.5. We merged the two reconstructions at the year 1845 (1845-1981 from PCA_{1845} and 1750-1844 from PCA_{1750}) for the final SWV (for southwest Virginia) reconstruction. We highlight that the BM chronology is determined for a single point, but that the SWV reconstruction is representative of the climate in the surrounding region as a result of being constructed from a PCA on growth series from sites spatially distributed around this point.

2.3 Climate data

We applied a two-tier approach to select the optimal climate target for reconstruction. In a first step, we used monthly climate values from the Blacksburg climate station (37 ° 12’ N, 80 ° 24’ W; elevation 634 m; 1901-2006) in a correlation function analysis with BM chronology. For this purpose, monthly precipitation sums

and average temperatures and PDSI values were computed from daily measurements.. Pearson's correlation coefficients were calculated for all months starting in April of the year previous to the growing season through current December, as well as for various seasons (Apr-June, July-Sep, Oct-Dec, Jan-Mar) and annual means. This analysis showed that the BM chronology was most strongly correlated with average May and June precipitation ($r=0.53$, $p<0.01$).

This result was then used in a second step as guidance for a spatial correlation analysis between the SWV chronology and a gridded (0.5 ° × 0.5 °) monthly climate data set for the period 1901-2006 [CRUTS3.10; 31]. Spatial correlations were calculated using the KNMI climate explorer [32; http://climexp.knmi.nl; Trouet and van Oldenborgh 2013]. The grid point showing the strongest correlation between the SWV chronology and May-June precipitation was then selected as a target for further climate-growth analysis and for reconstruction.

2.4 Reconstruction methods

Precipitation was modelled using a Bayesian linear regression model, with the first PCA chronology (1750-1981) as a predictor. The precipitation model is written as

$$y_t \sim Normal(\mu_t, \sigma^2) \quad (1)$$

$$\mu_t = \beta_0 + \beta_1 x_t, \quad (2)$$

where y_t represents precipitation values for the identified grid cell and x_t is the first PCA value at year t. Uninformative priors were placed on all three parameters as follows: $\beta_i \sim$ Normal(, 1000), and $\sigma^2 \sim$ Uniform(0, 100). Posterior distributions for all three parameters (β_0, β_1, and σ^2) were sampled using an adaptive Markov Chain Monte Carlo (MCMC) algorithm with a Metropolis step method, in which proposal distributions were adjusted accordingly when acceptance rates fell outside the ideal range of 0.2-0.5. The algorithm was run for 100,000 iterations with a burn-in of 50,000. Parameter estimates were thinned so that only every tenth estimate was saved to disk. The 0.025, 0.5 and 0.975 quantiles of these estimates were

determined to define an upper and lower bound for a 95% credible interval, as well as the median. At each iteration, parameter estimates were used to compute estimated precipitation. A 95% predictive interval was computed from these precipitation estimates using the 0.025, 0.5 and 0.975 quantiles. Note that frequentist methods could have been used with similar results, but we preferred the simple interpretation of the Bayesian credible interval.

2.5 Model calibration and verification

To assess the accuracy of the modeled precipitation anomalies, we used a split-period (1901-1941 and 1941-1981) calibration/verification scheme. Both the 1901-1940 and 1941-1981 periods of climate data were used in turn as the calibration period (denoted by y_t in 1), to determine if the accuracy of the reconstruction was sufficient to warrant further analysis. Data from the period not used for calibration served as verification data, and for both calibration/verification pairs we computed the mean squared error (MSE), reduction of error (RE) [12], coefficient of efficiency (CE) [33], and the squared correlation (r^2) (See the National Research Council report Surface Temperature Reconstructions for the Last 2,000 Years [34] for further details on assessing reconstruction skill).

2.6 Reconstruction analysis

We compared our precipitation reconstruction to six published regional precipitation and drought reconstructions as external validation (Table 3). One drought reconstruction was obtained from the North American Drought Atlas (NADA) [11], a tree-ring based gridded reconstruction of PDSI values for June through August over the last 2,000 years. The second drought reconstruction was a July PDSI reconstruction (JT) for Virginia and North Carolinian coastal regions [35]. The remaining four reconstructions identified for comparison were precipitation reconstructions for the North Carolina (NC), South Carolina (SC), and Georgia (GA) regions for the months of April though June for NC, and March through June for SC and GA [36], and one reconstruction for early summer anomalies for the Montpelier region (MP) [37].

Reconstructions that were significantly correlated with our reconstruction were compared using 31-year

window running correlations, which facilitated the identification of periods of pattern dissimilarity.

Furthermore, we used a spectral wavelet analysis to identify dominant cyclical behavior in our reconstruction [38]. Spectrum values were averaged with 2 frequencies per bin to simplify interpretation.

3 Results

The BM chronology covered the period 1764-2010 CE, had an interseries correlation of 0.556, and a mean sensitivity of 0.208 (Table 1). The EPS was higher than 0.85 for 1845-1981 and we thus used the chronology over this period. A spatial correlation analysis between climate variables and BM identified the grid point 37.5 - 38 ° N, 80.5 - 81 ° E as the location that correlated most strongly with our chronology (Fig. 3). The BM chronology was significantly positively correlated with monthly PDSI values from April of the previous year to December of the current year (Fig. 4B), except for previous May and previous October. We found particularly strong correlations between BM and monthly PDSI over the May through August growing season, with the highest correlation being with average June and July PDSI (jjPDSI; $r = 0.55$, $p < 0.01$). Furthermore, we found significant, positive correlations with precipitation of the previous year June and current year May and June (Fig. 4A). When averaging monthly precipitation values over the months May and June (mjPR), correlation increased to $r = 0.5$ ($p < 0.01$). The BM chronology did not correlate with monthly temperature values (Fig. 4C).

Based on this climate-growth analysis, mjPR and jjPDSI were considered as candidate targets for reconstruction. An assessment of the calibration/verification statistics for a reconstruction based on the BM chronology alone (results not shown), however, suggested that the climate signal was not sufficient to warrant adequate reconstruction skill. We therefore combined the BM chronology with four existing oak chronologies from nearby sites (Fig. 1, 2) in a nested PCA approach. All four chronologies were significantly positively correlated with the mjPR and jjPDSI values from the monthly data set obtained from the spatial correlation analysis (mjPR r: 0.38-0.55; jjPDSI r: 0.48-0.59; see Table 1).

The first PC axis ($PC1_{1845}$) of PCA_{1845} explained 57% of the common variance, with the second axis explaining 15.2%. All oak chronologies had a positive loading on $PC1_{1845}$, thus reflecting the correspondence between the time series. PC1 of the PCA_{1750} run ($PC1_{1750}$) explained 56% of the common variance and $PC2_{1750}$ explained 28.3%. $PC1_{1845}$ and $PC1_{1750}$ were strongly positively correlated over the period of overlap ($r = 0.93$, $p < 0.001$) and we merged the PC1 time series at the year 1845 (PCA_{1750}: 1750-1844, PCA_{1845}: 1845-1981) to form a single chronology extending from 1750 to 1981. This chronology will from hereon be named SWV (for southwest Virginia).

When comparing SWV with monthly climate variables, we generally find higher correlations than for the individually contributing tree-ring series (Fig. 3) and this is particularly true for mjPR ($r = 0.61$, $p < 0.01$) and jjPDSI ($r = 0.63$, $p < 0.01$). We thus tested mjPR and jjPDSI as potential reconstruction targets in a split calibration/verification scheme (Table 2). RE and CE values were negative for jjPDSI when using the later calibration period (1942-1981), indicating a poor fit of the reconstruction model. RE and CE are key statistics to determine the skill of a reconstruction, and our decision to reconstruct mjPR rather than jjPDSI was based on these values. Our final mjPR reconstruction, now referred to as rSWV, was scaled against the entire 1901-1981 interval. Estimates of rSWV and corresponding 95% predictive intervals were computed for each year of the period of reconstruction using posterior parameter draws (Fig. 5).

We compared rSWV to other regional moisture reconstructions (Table 4) and found positive correlations across the board. The strongest correlation was found with the NADA summer drought reconstruction ($r = 0.53$, $p < 0.01$), but we note that the LH chronology was used in the construction of both rSWV and NADA, thus implying that these records are not completely independent. A spectral analysis shows a periodicity in the rSWV reconstruction with peaks at 11, 17, and 24 years (Fig. 6).

4 Discussion

We investigated the relationship between climate and annual radial QUPR growth at a closed canopy site in the southeastern US. After removing the portion of the signal attributed to stand dynamics and intrinsic age trends, we found that early summer (May through June) moisture was the strongest positive influence on

radial growth. Similar climate-growth relationships have been identified by previous studies on oak in the southeastern US [15, 40] and can be explained by ecophysiological mechanisms. Radial growth of oak species typically starts in April or May after leaf-out and is 90% complete by the end of July even in years with adequate moisture [41]. In the first months of the growing season, carbon is allocated predominantly to radial thickening, whereas later in the season the focus of this allocation is shifted to carbohydrate storage [42]. Under severe moisture stress, oak carbon allocation is shifted from shoot to root, thereby increasing the root/shoot ratio [43]. QUPR is considered to be more tolerant to drought stress than other oak species and exhibits several morphological adaptations in order to better cope with moisture stress events [43]. However, we found that its radial growth was strongly influenced by moisture availability, suggesting that in years with inadequate moisture, radial growth is not a priority and carbon allocation is likely focused on maintenance or root development. The identifiable moisture response in the detrended BM chronology demonstrates that oaks in a closed-canopy forest can be used as paleoclimate proxies if the non-climatic portion of the low-frequency signal in the tree-ring time series is removed with great care [44, 45]. The development of a biologically motivated trend removal algorithm may improve current practices in dendroclimatology [46]. In addition, care must be taken in closed canopy forests when attempting to use growth series as proxy records as younger stands in the stem-exclusion phase may be dominated by the effects of competition rather than of climate [47].

To isolate and strengthen the moisture-growth relationship of the BM chronology, we performed a nested PCA including five regional summer moisture sensitive *Quercus* chronologies. The spatial pattern of the relationship between the resulting SWV chronology and early summer precipitation indicates that SWV is positively correlated with moisture in the Great Appalachian Valley (Figure 3). Mountains play an important role in the hydrological cycle for several reasons, one of which being that they are the points of origin of most rivers [48]. Increases in precipitation in mountainous regions leads to increased stream flow volumes and surface runoff, which in turn increases soil moisture in the Appalachian watershed.

Our reconstruction generally shows similar variability as other reconstructions of moisture variability in the southeastern US (Table 4) The strongest similarity was found with the NADA PDSI reconstruction

(Figure 7), but we note the lack of full independence between these two records. Despite the overall strong agreement between both records, a 31-year windowed correlation between rSWV and NADA PDSI indicated that these records were not consistent for the period 1853-1866.

All five chronologies contributing to SWV show a pattern of reduced correlation with the NADA PDSI reconstruction during this period, which coincides with a La Niña event ocurring from 1855-1863 [49]. La Niña events typically have strong impacts on the West Coast, but affect weather patterns throughout North America, and have even been shown to affect the Atlantic hurricane season [50]. During this large-scale ocean-atmosphere phenomenon, temperature anomalies in the southeastern US [XXX] in combination with low moisture availability likely led to a change in the otherwise stationary precipitation-growth relationship.

The rSWV reconstruction showed anomalies consistent with the instrumental precipitation record for 1901-1981 (Figure 3). In particular, the reconstruction correctly identifies the severe nation-wide dust bowl era drought in the 1930s as well as the drought year 1956, the single worst drought year of the 1950s drought [51]. However, when compared at a decadal scale after application of a 10-year smoothing spline, the rSWV reconstruction and instrumental record are less consistent before 1950 (Figure 5). This is likely a result of the changing variability in the reconstruction – in some periods the reconstruction is quite variable as seen by the exaggerated response to extreme precipitation values, while in other periods there is less variability and this response is less exaggerated. This is indicative that the trees are either responding to a combination of other factors or are experiencing inconsistent lagged precipitation effects.

In years prior to the instrumental record, the rSWV reconstruction identifies several dry periods in 1760-1776, 1867-1874, and 1894-1902. There is evidence of a dry period from 1984-1902 in the NADA, JT, and MP reconstructions. The other dry periods are less pronounced in the compared drought or precipitation reconstructions, or are not apparent.

The rSWV reconstruction shows an 11-year cyclicity (Figure 6), a periodicity that has been observed in both instrumental and paleo-reconstructed temperature and moisture indices, such as the Northern Hemisphere annual average land air temperature record extending from 1951-1980, the Northern Hemisphere annual

temperature anomalies reconstructed from proxy data for 1579-1880, as well as for many of the contiguous states using state-averaged instrumental temperature and precipitation records [52, 53]. In particular, this cyclic pattern has been identified in June precipitation in the southeastern US [52], but was not apparent in western US tree-ring based PDSI reconstructions [54]. This observed 11-year periodicity is a characteristic of the solar cycle, which has been shown to be reflected in terrestrial climate, and identified as one of the contributing factors that determine global temperature [53, 55, 56]. Solar periods of high and low activity can be measured by the number of sunspots or the solar cycle length [57, 58]. A larger number of sunspots indicates greater solar activity, and the magnetic fields in these sunspots have the ability to release large amounts of stored energy as solar flares or coronal mass ejections. These changes in released energy in turn affect the realized weather patterns. Studies have shown that these changes in released energy may also influence hydroclimate [52, 59]. However, despite the presence of strong correlations between terrestrial climate records and solar cycles, physical mechanisms that explain the effects of external solar forcing on global circulation patterns have yet to be fully understood [60].

We have shown that QUPR growth in the southern Appalachians is positively influenced by early summer precipitation and we successfully reconstructed May-June precipitation for the period 1750-1981 and thus extended the instrumental record with150 years. Long records of climatic variability and its influence on ecosystems are particularly important in the Southern Appalachians, one of the most biologically diverse temperate forest systems.Extending the climate record will allow scientists to have more information as to how climate affects tree growth and shapes ecosystems. This will better prepare us for predicting future vegetation changes that may occur with a changing climate. This region has supported continuous forest communities longer than any other area on the North American continent, and hosts many rare, endemic species [1]. Additionally, it harbors many disjunct species populations. The southern Appalachians also provide ecosystem services such as carbon storage, watershed and water quality protection, and serve as a timber source [2]. Understanding past climate-ecosystem relationships in this region will enable scientists and landowners to better manage natural resources in our current changing climate

5 Acknowledgements

The authors would like to thank the North American Dendroecological Fieldweek (NADEF) Dendroclimatology group for assisting with data collection, and Carolyn Copenheaver for assisting with site selection. We would also like to thank the organizers of NADEF, especially Jim Speer.

Chron	Lat (N), Long (W)	SIC	MS	N	MSL	mjPR	jjPDSI	Period	Citation
BM	37.37, 80.24	0.556	0.208	76	128.3	0.50*	0.55*	1845 - 2010	This study
LH	35.62, 85.43	0.609	0.171	19	181.4	0.55*	0.48*	1750 - 1997	Stahle, D.W. & Therrell, M.D. 2005
WD	38.50, 78.35	0.523	0.163	26	250.8	0.43*	0.59*	1735 - 1981	Cook, E.R. 1994
CC	37.35, 80.37	0.592	0.218	20	194.1	0.38*	0.50*	1800 - 2001	Copenheaver, C.A. 2010
OC	39.88, 76.40	0.575	0.169	18	260.2	0.24**	0.19	1745 - 1981	Cook, E.R. 1994

Table 1: Site-specific details for the Brush Mountain (BM), Lynn Hollow (LH), Watchdog Mountain (WD), Craig Creek (CC), and Otter Creek (CC) sites, including location, series intercorrelation (SIC), mean sensitivity (MS), number of series (N), mean segment length (MSL), correlations between the chronology with both the averaged May-June precipitation (mjPR) and averaged June-July PDSI (jjPDSI), the period for which the EPS is greater than 0.85, and the data citation. All correlation statistics between the chronologies and the weather data were significant ($p < 0.01$ indicated by *, $p < 0.05$ indicated by **), except for one ($p = 0.19$).

	Calibration			
	mjPR		jjPDSI	
	1901-1941	1942-1981	1901-1941	1942-1981
RE	0.10 (0.20)	0.30 (0.42)	0.44 (0.26)	-0.41 (-0.66)
CE	0.10 (0.19)	0.30 (0.41)	0.39 (0.20)	-0.60 (-0.88)
Calibration R^2	0.64 (0.75)	0.56 (0.55)	0.58 (0.62)	0.74 (0.59)
Verification R^2	0.56 (0.55)	0.64 (0.75)	0.74 (0.59)	0.59 (0.62)

Table 2: rSWV and PCA_{1750} (in brackets) reconstruction skill statistics for mjPR and jjPDSI. Statistics include the reduction of error (RE), coefficient of efficiency (CE), and the calibration and verification period R^2.

Site	Location	Variable	Range (years)	Data type	Variance explained (R^2) [A]
NADA [11]	37° 30’ N, 80° 0’ W VA	Jun-Aug PDSI	1185-2006	Tree rings	0.55*
JT [35]	Coastal NC and VA	July PDSI	1700-1984	Tree rings	0.44
NC [36]	Statewide NC	Apr-Jun precip	933-1985	Tree rings	0.54
SC [36]	Statewide SC	Mar-Jun precip	1005-1985	Tree rings	0.58
GA [36]	Statewide GA	Mar-Jun precip	933-1985	Tree rings	0.68
MP [37]	38° 13’ N, 78° 10’ W; VA	Early summer precip	1784-1966	Tree rings & Meteorological diary	0.39

[A] R^2 values as reported in cited references; may or may not be adjusted.

* Median value of R^2 for all gridpoints in the PDSI reconstruction grid (see [11]).

Table 3: Details for the six southeastern US moisture reconstructions compared to the rSWV reconstruction. This table should come before the previous table.

	Recon	PDSI		Precip			
	rSWV	JT	NADA	NC	SC	GA	MP[A]
rSWV	1						
JT	0.215*	1					
NADA	0.593*	0.502*	1				
NC	0.227*	0.396*	0.424*	1			
SC	0.118	0.178*	0.352*	0.581*	1		
GA	0.079	0.196*	0.345*	0.474*	0.766*	1	
MP[A]	0.378*	0.288*	0.499*	0.132	0.090	0.109	1

Table 4: Annual correlation (1750-1981) between the rSWV reconstruction and other reconstructions including the NADA and JT drought reconstructions; and the NC, SC, GA, and MP precipitation reconstructions. All values indicated by * indicate significant correlations at the $p < 0.01$ level.
[A] Reconstruction covers only the period 1764 - 1966.

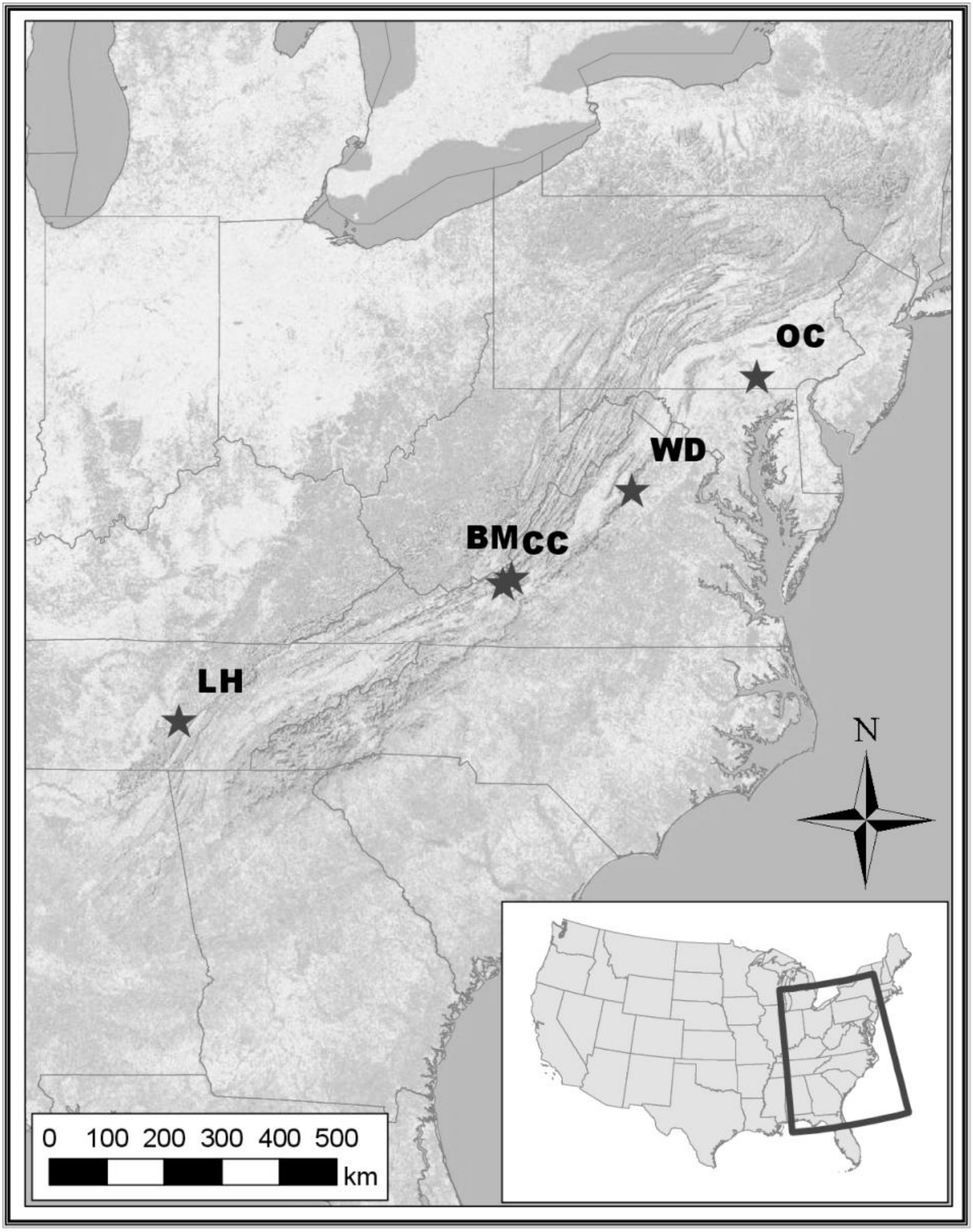

Figure 1: Regional chronology sample locations.

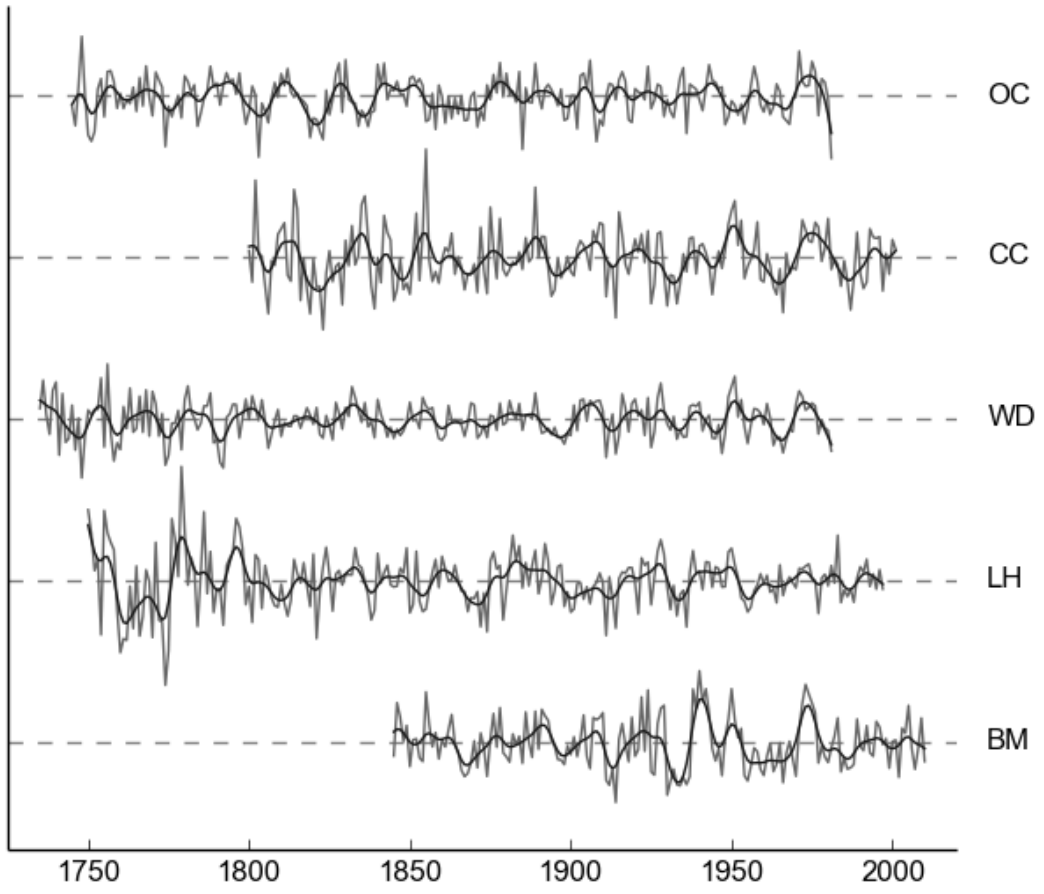

Figure 2: The five chronologies used in PCA_{1850}. The top panel shows the chronology built from the sample data at Brush Mountain (BM), while the others are the regional chronologies from Lynn Hollow (LH), Watchdog Mountain (WD), Craig Creek (CC), and Otter Creek (OC).

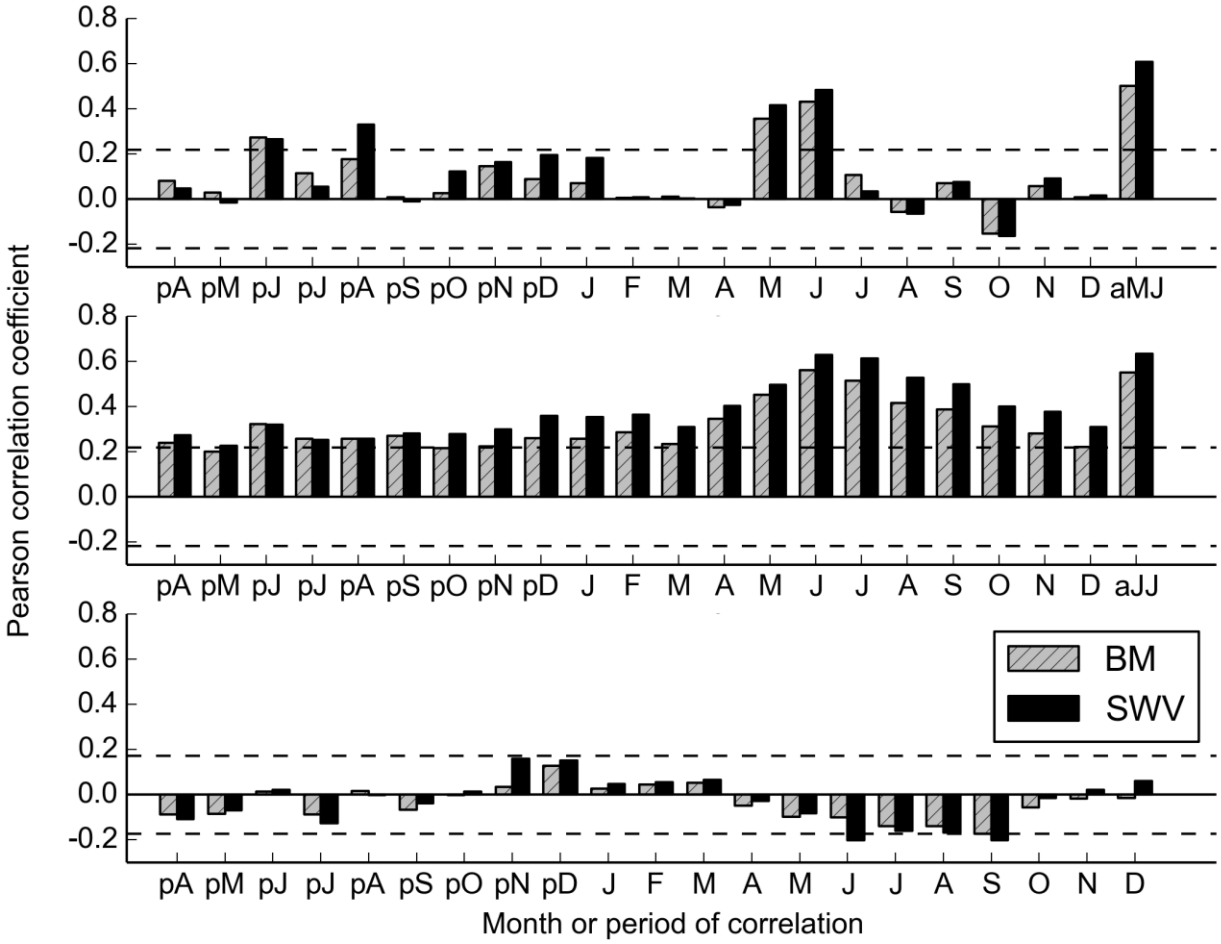

Figure 4: Correlation between the BM and SWV chronologies and the gridded (Top) monthly precipitation from previous April (pA) through December (D) as well as for average May and June (aMJ); (Center) average PDSI from previous April (pA) through December (D) as well as for average June and July (aJJ); and (bottom) average monthly temperature from previous April (pA) through December (D).

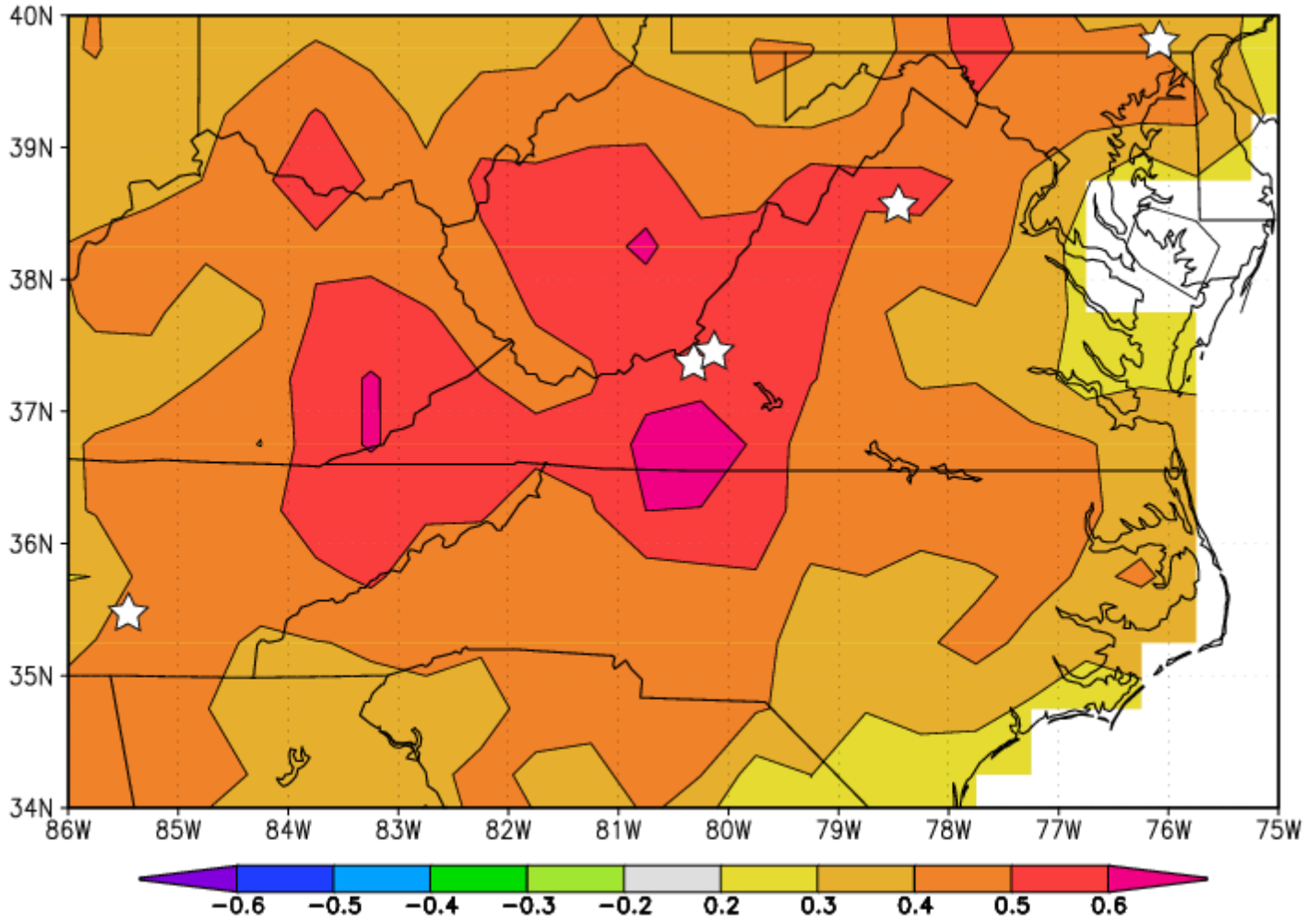

Figure 3: Correlation map (1901-1981) between the SWV chronology and gridded average May-June precipitation (CRUTS3.10). Stars indicate the PCA_{1850} tree-ring site locations.

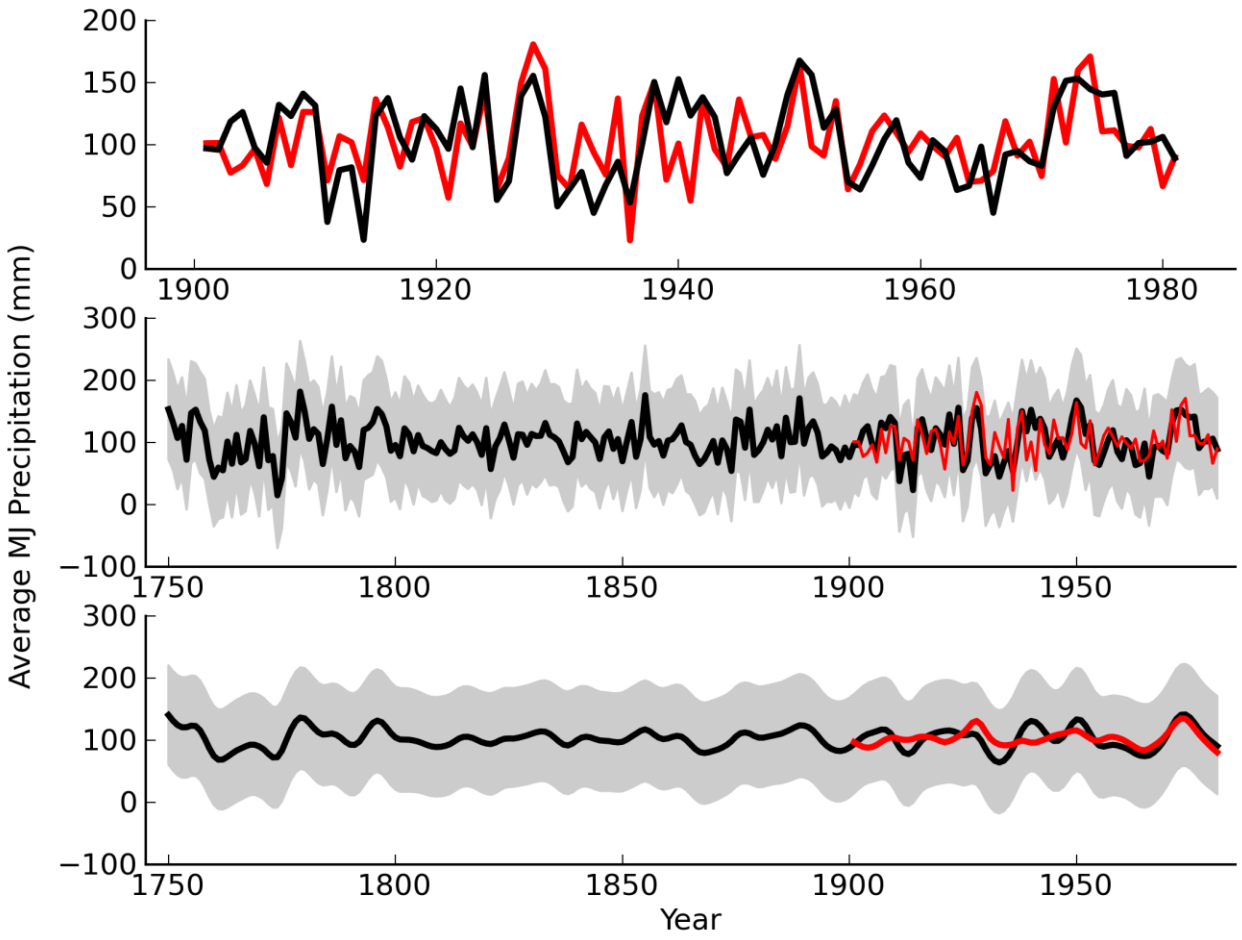

Figure 5: Top panel: rSWV reconstruction (black curve) and the average May-June precipitation (red curve; 1901-1981). Middle panel: rSWV reconstruction (black curve), 95% credibility interval (shaded grey area), and average May-June precipitation (red curve) for the 1750-1981 period of reconstruction. Bottom panel: Smoothed (10-year) rSWV reconstruction (black curve), 95% credible interval (shaded grey area), and average May-June precipitation (red curve). Smoothing performed using a 10-year smoothing spline to highlight decadal-scale variability.

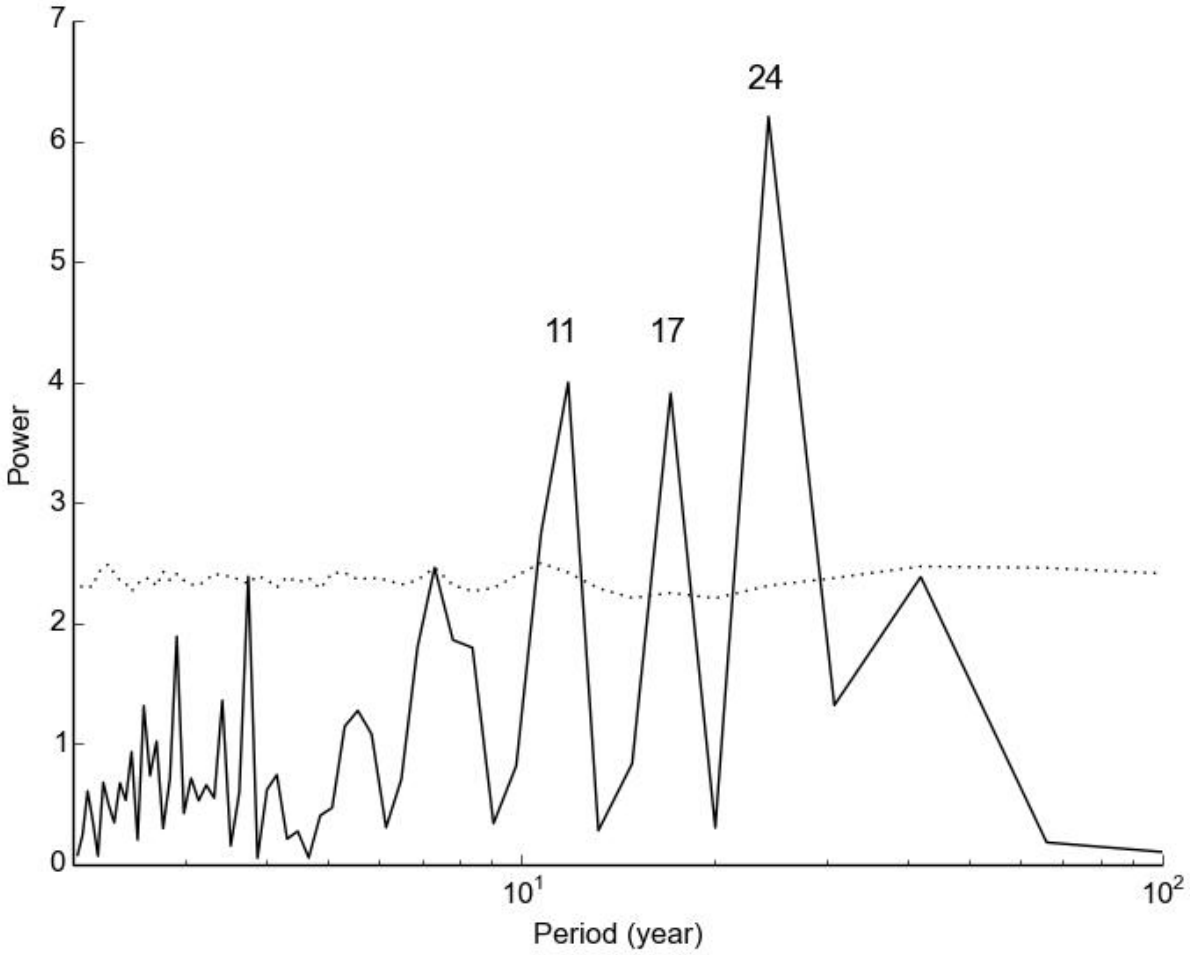

Figure 6: Periodogram of the SWV reconstruction showing spectral power peaks at approximately 11, 17, and 24 years.

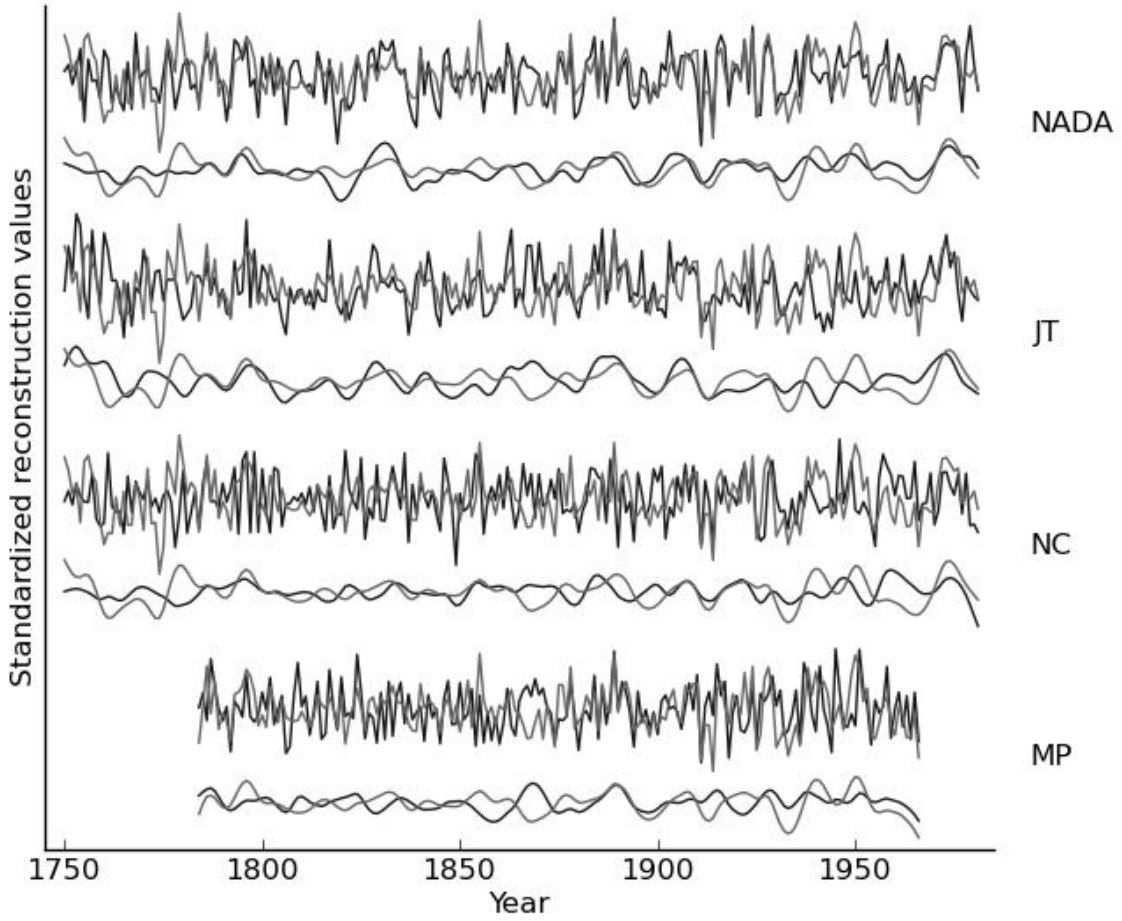

Figure 7: The standardized rSWV average May-June precipitation reconstruction (grey lines) is plotted on top of the other moisture reconstructions (NADA, JT, NC, and MP; black lines) which were significantly correlated to rSWV. Standardized reconstructions are shown at an annual scale and at a decadal-scale obtained by application of a 10-year smoothing spline. Particularly notable differences between rSWV and the other reconstructions are the year 1774 and the interval 1863-1872.

References

[1] North Carolina Natural Heritage Program (NCNHP). An Inventory of the Significant Natural Areas of Ashe County, North Carolina, 1999. URL http://www.ncnhp.org/Images/Ashe10-_10-_2005.pdf. Accessed September 2012.

[2] C.E. Zipper, J.A. Burger, J.G. Skousen, P.N. Angel, C.D. Barton, V. Davis, and J.A. Franklin. Restoring forests and associated ecosystem services on appalachian coal surface mines. *Environmental management*, 47(5):751–765, 2011.

[3] RK Pachauri and A. Reisinger. Climate Change 2007: Synthesis Report. Contribution of Working Groups I, II and III to the Fourth Assessment Report of the Intergovernmental Panel on Climate Change. *Intergovernmental Panel on Climate Change*, 2007.

[4] K. Kattenberg, F. Giorgi, H. Grassl, G.A. Meehl, J.F.B. Mitchell, R.J. Stouffer, T. Tokioka, A.J. Weaver, and T.M.L Wigley. Climate models–projections of future climate. In J.T. Houghton, LG Meiro Filho, B.A. Callander, N. Harris, A. Kattenburg, and K. Maskell, editors, *Climate change 1995: The science of climate change: contribution of working group I to the second assessment report of the Intergovernmental Panel on Climate Change*, pages 285–357. Cambridge University Press, 1996.

[5] R. Seager, A. Tzanova, and J. Nakamura. Drought in the southeastern United States: Causes, variability over the last millennium, and the potential for future hydroclimate change. *Journal of Climate*, 22(19):5021–5045, 2009.

[6] S. Sobolowski and T. Pavelsky. Evaluation of present and future North American Regional Climate Change Assessment Program (NARCCAP) regional climate simulations over the southeast United States. *Journal of Geophysical Research*, 117:D01101, 2012.

[7] E.R. Cook, C.A. Woodhouse, C.M. Eakin, D.M. Meko, and D.W. Stahle. Long-term aridity changes in the western United States. *Science*, 306(5698):1015–1018, 2004.

[8] U. Büntgen, D.C. Frank, R.J. Kaczka, A. Verstege, T. Zwijacz-Kozica, and J. Esper. Growth responses to climate in a multi-species tree-ring network in the Western Carpathian Tatra Mountains, Poland and Slovakia. *Tree Physiology*, 27(5):689–702, 2007.

[9] D.C. LeBlanc. Temporal and spatial variation of oak growth-climate relationships along a pollution gradient in the midwestern United States. *Canadian Journal of Forest Research*, 23 (5):772–782, 1993.

[10] D.W. Stahle and M.K. Cleveland. Large-scale climatic influences on baldcypress tree growth across the southeastern united states. In P.D. Jones, R.S. Bradley, and J. Jouzel, editors, *Climatic variations and forcing mechanisms of the last 2000 years*, I41, pages 125 – 140. NATO ASI, 1993.

[11] E.R. Cook, D.M. Meko, D.W. Stahle, and M.K. Cleaveland. Drought reconstructions for the continental United States. *Journal of Climate*, 12(4):1145–1162, 1999.

[12] H.C. Fritts. *Tree rings and climate*. London, New York, San Francisco.: Academic Press, 1976.

[13] R.L. Phipps. Comments on interpretation of climatic information from tree rings, eastern North America. *Tree-ring bulletin*, 42:11–22, 1982.

[14] C. Pan, SJ Tajchman, and JN Kochenderfer. Dendroclimatological analysis of major forest species of the central Appalachians. *Forest Ecology and Management*, 98(1):77–87, 1997.

[15] J.H. Speer, H.D. Grissino-Mayer, K.H. Orvis, and C.H. Greenberg. Climate response of five oak species in the eastern deciduous forest of the southern Appalachian Mountains, USA. *Canadian Journal of Forest Research*, 39(3):507–518, 2009.

[16] D.L. Rubino and B.C. McCarthy. Dendroclimatological analysis of white oak (*Quercus alba* L., Fagaceae) from an old-growth forest of southeastern Ohio, USA. *Journal of the Torrey Botanical Society*, pages 240–250, 2000.

[17] M.A. Stokes and T.L. Smiley. *An introduction to tree-ring dating*. University of Arizona Press, 1996.

[18] David K Yamaguchi. A simple method for cross-dating increment cores from living trees. *Canadian Journal of Forest Research*, 21(3):414–416, 1991.

[19] R.L. Holmes. Computer-assisted quality control in tree-ring dating and measurement. *Tree-ring bulletin*, 43(1):69–78, 1983.

[20] E.R. Cook and K. Peters. Calculating unbiased tree-ring indices for the study of climatic and environmental change. *The Holocene*, 7(3):361–370, 1997.

[21] E.R. Cook and K. Peters. The smoothing spline: a new approach to standardizing forest interior tree-ring width series for dendroclimatic studies. *Tree-ring bulletin*, 41:45–53, 1981.

[22] R.A. Monserud. Time-series analyses of tree-ring chronologies. *Forest Science*, 32(2): 349–372, 1986.

[23] E.R. Cook. The decomposition of tree-ring series for environmental studies. *Tree-Ring Bulletin*, 47:37–59, 1987.

[24] TML Wigley, KR Briffa, and PD Jones. On the average value of correlated time series, with applications in dendroclimatology and hydrometeorology. *Journal of Climate and Applied Meteorology*, 23(2):201–213, 1984.

[25] K. Peters, GC Jacoby, and E.R. Cook. Principal components analysis of tree-ring sites. *Tree-Ring Bulletin*, 41:1–19, 1981.

[26] KJ Anchukaitis, MN Evans, A. Kaplan, EA Vaganov, MK Hughes, HD Grissino-Mayer, and MA Cane. Forward modeling of regional scale tree-ring patterns in the southeastern United States and the recent influence of summer drought. *Geophysical Research Letters*, 33(4):L04705, 2006.

[27] G.C. Jacoby and R. D'Arrigo. Reconstructed northern hemisphere annual temperature since 1671 based on high-latitude tree-ring data from North America. *Climatic Change*, 14(1): 39–59, 1989.

[28] S. Wold, K. Esbensen, and P. Geladi. Principal component analysis. *Chemometrics and intelligent laboratory systems*, 2(1):37–52, 1987.

[29] Edward R Cook, Richard Seager, Mark A Cane, and David W Stahle. North american drought: reconstructions, causes, and consequences. *Earth-Science Reviews*, 81(1):93–134, 2007.

[30] Wayne C Palmer. *Meteorological drought*. US Department of Commerce, Weather Bureau Washington, DC, USA, 1965.

[31] I. Harris, P.D. Jones, T.J. Osborn, and D.H. Lister. Updated high-resolution grids of monthly climatic observations–the CRU TS3. 10 dataset. *International Journal of Climatology*, 34(3):623–642, 2014.

[32] V. Trouet and G.J. Van Oldenborgh. KNMI Climate Explorer: a web-based research tool for high-resolution paleoclimatology. *Tree-Ring Research*, 69(1):3–13, 2013.

[33] Edward R Cook, Keith R Briffa, and Philip D Jones. Spatial regression methods in dendroclimatology: a review and comparison of two techniques. *International Journal of Climatology*, 14(4):379–402, 1994.

[34] National Research Council Committee on Surface Temperature Reconstructions for the Last 2, 000 Years. *Surface Temperature Reconstructions for the Last 2,000 Years*. The National Academies Press, 2006.

[35] D.W. Stahle, M.K. Cleaveland, D.B. Blanton, M.D. Therrell, and D.A. Gay. The lost colony and Jamestown droughts. *Science*, 280(5363):564–567, 1998.

[36] D.W. Stahle and M.K. Cleaveland. Reconstruction and analysis of spring rainfall over the southeastern US for the past 1000 years. *Bulletin of the American Meteorological Society;(United States)*, 73(12), 1992.

[37] D.L. Druckenbrod, M.E. Mann, D.W. Stahle, M.K. Cleaveland, M.D. Therrell, and H.H. Shugart. Late-eighteenth-century precipitation reconstructions from James Madison's Montpelier plantation. *Bulletin of the American Meteorological Society*, 84(1):57–72, 2003.

[38] C. Torrence and G.P. Compo. A practical guide to wavelet analysis. *Bulletin of the American Meteorological society*, 79(1):61–78, 1998.

[39] HC Fritts, J. Guiot, GA Gordon, and F. Schweingruber. Methods of calibration, verification, and reconstruction. *Methods of Dendrochronology*, pages 163–217, 1990.

[40] Y. Li. *Dendroclimatic Analysis of Climate Oscillations for the Southeastern United States from Tree-ring Network Data*. PhD thesis, University of Tennessee, 2011.

[41] P.A. Robertson. Factors affecting tree growth on three lowland sites in southern Illinois. *American Midland Naturalist*, pages 218–236, 1992.

[42] R. Zweifel, L. Zimmermann, F. Zeugin, and D.M. Newbery. Intra-annual radial growth and water relations of trees: implications towards a growth mechanism. *Journal of Experimental Botany*, 57(6):1445–

1459, 2006.

[43] RE Dickson and PT Tomlinson. Oak growth, development and carbon metabolism in response to water stress. In *Annales des Sciences Forestières*, volume 53, pages 181–196, 1996.

[44] Edward Roger Cook. *A TIME SERIES ANALYSIS APPROACH TO TREE RING STANDARDIZATION*. PhD thesis, The University of Arizona, 1985.

[45] E R Cook, K Briffa, S Shiyatov, and V Mazepa. Tree-ring standardization and growth-trend estimation. In Edward R Cook and Leonardas A Kairiukstis, editors, *Methods of dendrochronology: applications in the environmental sciences*. Kluwer, 1990.

[46] Thomas M Melvin and Keith R Briffa. A "signal-free" approach to dendroclimatic standardisation. *Dendrochronologia*, 26(2):71–86, 2008.

[47] C.D. Oliver. Forest development in North America following major disturbances. *Forest ecology and management*, 3:153–168, 1980.

[48] M. Beniston, HF Diaz, and RS Bradley. Climatic change at high elevation sites: an overview. *Climatic Change*, 36(3):233–251, 1997.

[49] Julia E Cole, Jonathan T Overpeck, and Edward R Cook. Multiyear la niña events and persistent drought in the contiguous united states. *Geophysical Research Letters*, 29(13):25–1, 2002.

[50] R.A. Pielke Jr and C.N. Landsea. La niña, el niño and atlantic hurricane damages in the United States. *Bulletin of the American Meteorological Society*, 80(10):2027–2033, 1999.

[50] National Oceanic and Atmosheric Administration (NOAA), Climate Prediction Center (CPC). El Niño Southern Oscillation (ENSO), 2005. URL http://www.cpc.ncep.noaa.gov/products/precip/CWlink/MJO/enso.shtml. Accessed September 2014.

[51] Falko K Fye, David W Stahle, and Edward R Cook. Paleoclimatic analogs to twentieth-century moisture regimes across the united states. *Bulletin of the American Meteorological Society*, 84(7):901–909, 2003.

[52] D.J. Hancock and D.N. Yarger. Cross-spectral analysis of sunspots and monthly mean temperature and precipitation for the contiguous United States. *Journal of Atmospheric Sciences*, 36:746–746, 1979.

[53] K. Lassen and E. Friis-Christensen. Variability of the solar cycle length during the past five centuries and the apparent association with terrestrial climate. *Journal of Atmospheric and Terrestrial Physics*, 57(8):835–845, 1995.

[54] E.R. Cook, D.M. Meko, and C.W. Stockton. A new assessment of possible solar and lunar forcing of the bidecadal drought rhythm in the western United States. *Journal of Climate*, 10 (6):1343–1356, 1997.

[55] G.C. Reid. Solar irradiance variations and the global sea surface temperature record. *Climate Change:*

Natural forcing factors for climate change timescales 10-1 to 10-5 years, 2:7, 2002.

[56] National Research Council Board on Global Change. *Solar Influences on Global Change*. The National Academies Press, 1994. ISBN 9780309051484. URL http://www.nap.edu/openbook.php?record_id=4778.

[57] Eigil Friis-Christensen and Knud Lassen. Length of the solar cycle- an indicator of solar activity closely associated with climate. *Science*, 254(5032):698–700, 1991.

[58] Ilya G Usoskin, Sami K Solanki, Manfred Schüssler, Kalevi Mursula, and Katja Alanko. Millennium-scale sunspot number reconstruction: Evidence for an unusually active sun since the 1940s. *Physical Review Letters*, 91(21):211101, 2003.

[59] J.E. Nichols and Y. Huang. Hydroclimate of the northeastern United States is highly sensitive to solar forcing. *Geophysical Research Letters*, 39(4):L04707, 2012.

[60] S.W. Franks. Assessing hydrological change: deterministic general circulation models or spurious solar correlation? *Hydrological Processes*, 16(2):559–564, 2002.

[61] R.A. Warrick et al. Drought in the great plains: A case study of research on climate and society in the USA. *Climatic constraints and human activities*, 10:93–123, 1980.

[62] C.M. Ruffner and M.D. Abrams. Relating land-use history and climate to the dendroecology of a 326-year-old *Quercus prinus* talus slope forest. *Canadian Journal of Forest Research*, 28(3):347–358, 1998.

[63] State of California. Drought conditions in California. Technical report, Department of Water Resources, 1990.

[64] M.P. Lawson and C.W. Stockton. Desert myth and climatic reality. *Annals of the Association of American Geographers*, 71(4):527–535, 2005.